

Original Article

Cite this article: Zhu Y-S, Yang J-H, Wang H, and Wu F-Y (2019) A Palaeoproterozoic basement beneath the Rangnim Massif revealed by the *in situ* U–Pb ages and Hf isotopes of xenocrystic zircons from Triassic kimberlites of North Korea. *Geological Magazine* **156**: 1657–1667. <https://doi.org/10.1017/S0016756818000900>

Received: 7 April 2018

Revised: 29 November 2018

Accepted: 3 December 2018


First published online: 9 January 2019

Keywords:

kimberlite; Rangnim Massif; North Korea; zircon Hf isotopes; zircon U–Pb ages

Author for correspondence: Yu-Sheng Zhu, Email: zhuyusheng@mail.iggcas.ac.cn

A Palaeoproterozoic basement beneath the Rangnim Massif revealed by the *in situ* U–Pb ages and Hf isotopes of xenocrystic zircons from Triassic kimberlites of North Korea

Yu-Sheng Zhu^{1,2} , Jin-Hui Yang^{1,2,3}, Hao Wang^{1,2} and Fu-Yuan Wu^{1,2,3}

¹State Key Laboratory of Lithospheric Evolution, Institute of Geology and Geophysics, Chinese Academy of Sciences, Beijing 100029, China; ²Institutions of Earth Science, Chinese Academy of Sciences, Beijing 100029, China and ³University of Chinese Academy of Sciences, Beijing 100049, China

Abstract

In situ U–Pb and Hf analyses were used for crustal zircon xenocrysts from Triassic kimberlites exposed in the Rangnim Massif of North Korea to identify components of the basement hidden in the deep crust of the Rangnim Massif and to clarify the crustal evolution of the massif. The U–Pb age spectrum of the zircons has a prominent population at 1.9–1.8 Ga and a lack of Archaean ages. The data indicate that the deep crust and basement beneath the Rangnim Massif are predominantly of Palaeoproterozoic age, consistent with the ages of widely exposed Palaeoproterozoic granitic rocks. *In situ* zircon Hf isotope data show that most of the Palaeoproterozoic zircon xenocrysts have negative $\varepsilon_{\text{Hf}}(t)$ values (–9.7 to +0.7) with an average Hf model age of 2.86 ± 0.02 Ga (2σ), which suggests that the Palaeoproterozoic basement was not juvenile but derived from the reworking of Archaean rocks. Considering the existence of Archaean remanent material in the Rangnim Massif and their juvenile features, a strong crustal reworking event is indicated at 1.9–1.8 Ga, during which time the pre-existing Archaean basement was exhausted and replaced by a newly formed Palaeoproterozoic basement. These features suggest that the Rangnim Massif constitutes the eastern extension of the Palaeoproterozoic Liao–Ji Belt of the North China Craton instead of the Archaean Liaonan Block as previously thought. A huge Palaeoproterozoic orogen may exist in the eastern margin of the Sino-Korean Craton.

1. Introduction

The Sino-Korean Craton is one of the most ancient in the world and consists primarily of the North China Craton (NCC) in China and the Rangnim Massif in North Korea (Fig. 1). Various studies have revealed that the Precambrian basement of the NCC is dominated by late Archaean (2.8–2.5 Ga) tonalite–trondhjemite–granodiorite (TTG) gneisses and supracrustal rocks, with minor amounts of early and middle Archaean components (Zhao & Zhai, 2013). However, because of the difficulties in accessing rock outcrops and obtaining rock samples, the characteristics and tectonic affinity of the basement beneath the Rangnim Massif remain controversial. Based on a few early late Archaean and Proterozoic ages yielded by whole-rock Sm–Nd and Rb–Sr isochron methods, the crustal basement of the Rangnim Massif has been thought to be connected to the NCC and characterized by widely exposed Archaean rocks (Huang, 1977; Paek *et al.* 1996, p. 619; Qiao & Zhang, 2002). This viewpoint has recently gained support from the high-precision U–Pb dating of zircons, which has yielded ages of 2.64–2.51 Ga for the granitoids that occur mainly along the eastern and southern margins of the Rangnim Massif (Zhao *et al.* 2006, 2016a; Zhang *et al.* 2016). However, detrital zircons collected from sands in the major rivers that traverse North Korea indicate another scenario, given that their ages cluster dominantly around 1.9–1.8 Ga and there are fewer Archaean ages (Wu *et al.* 2007b, 2016). Similarly, most of the Precambrian plutonic rocks exposed in the Rangnim Massif have crystallization ages of 1.9–1.8 Ga (Peng *et al.* 2016). Archaean rocks are limited in scale and are distributed only locally along the southern and eastern margins of the massif. These observations argue for a Palaeoproterozoic-dominated basement beneath the Rangnim Massif, with Archaean rocks being restricted to small isolated remnants within the Palaeoproterozoic terrane (Wu *et al.* 2016).

The arguments summarized above for different viewpoints are derived mainly from observations obtained from the shallow crustal layer, and they lack any consideration of the nature of the hidden crust that constitutes most of the basement. This lack of information about the true nature of the crustal components may result in biased or false conclusions (e.g. Zheng *et al.* 2006; Donatti-Filho *et al.* 2013). If we are to constrain the formation and evolution of the Rangnim Massif, further information on the deep structure of the basement is therefore required, especially for those regions where Archaean rocks are exposed.

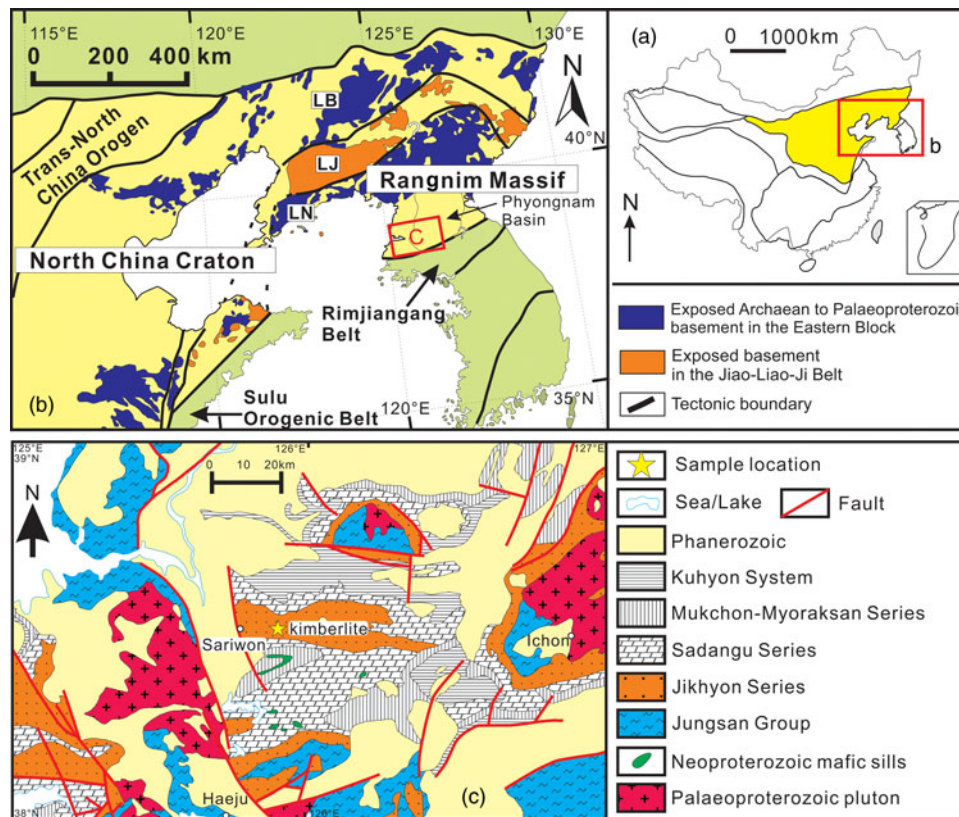


Fig. 1. (Colour online) (a) The location of the Sino-Korean Craton and (b) a regional geological map of Precambrian rocks in the eastern NCC and Rangnim Massif, modified after Zhao & Zhai (2013). LB – Liaobei Block; LN – Liaonan Block; LJ – Liao–Ji mobile belt. (c) Geological sketch map of Precambrian rocks in the Phyonngnam Basin in the southern region of the Rangnim Massif. The location of the kimberlite samples is shown. The map is modified after Paek *et al.* (1996).

Kimberlites are well known within Precambrian terranes and include the Kaapvaal Craton, the Siberian Craton and the NCC (e.g. Zheng *et al.* 2009; Sparks, 2013; Sun *et al.* 2014). Kimberlites commonly form at great depths and are transported rapidly from the mantle to the Earth's surface (Wyllie, 1980; Mitchell, 1986; Kelley & Wartho, 2000). During their ascent, the kimberlitic magmas may interact with the lithosphere and capture mantle and/or crustal xenoliths or xenocrysts that provide information about the nature of cryptic components in the lithospheric mantle and crust during the time of the kimberlitic eruption (e.g. Rollinson, 1997; Zheng *et al.* 2007; Ashchepkov *et al.* 2012). Zircon xenocrysts are of special interest because they provide not only accurate U–Pb age data, but also information on whether the zircons crystallized from juvenile or recycled sources, as revealed by their Hf isotopes (Kinny & Maas, 2003; Kemp *et al.* 2006). The integration of U–Pb dating and Hf isotope data for xenocrystic zircons can therefore be used to characterize the vertical section of the lithosphere segment through which the kimberlitic magma passed, thus revealing its secular and variable evolution. In combination with data on the rocks exposed at the surface, the data from xenocrystic zircons could provide more comprehensive and reliable constraints on the nature and tectonic affinity of an otherwise little-known massif (e.g. Batumike *et al.* 2007; Zheng *et al.* 2009; Donatti-Filho *et al.* 2013; Kostrovitsky *et al.* 2016).

Several Triassic kimberlite pipes and dykes are exposed within the Rangnim Massif (Fig. 1c; Yang *et al.* 2010), and these hypabyssal rocks contain abundant zircon xenocrysts, thus providing a useful way of probing the deep lithospheric structure of the Rangnim Massif. In this paper, we explain how *in situ* U–Pb dating and Hf isotope analyses of zircon xenocrysts in the kimberlites of

North Korea are able to reveal the age structure of the basement beneath the Rangnim Massif, constrain the crustal evolution of North Korea and provide further insights into the tectonic affinity of the Rangnim Massif.

2. Geological setting

North Korea consists of two major tectonic units: the Rangnim Massif and the Rimjingang Belt (Fig. 1b). The Rimjingang Belt, located on the southern side of North Korea, is characterized by high-pressure eclogites and gneisses, and it has been considered to be the eastern extension of the Dabie–Sulu ultra-high-pressure belt (Yin & Nie, 1993; Ree *et al.* 1996; Kwon *et al.* 2009), which resulted from the collision of the north and south China continents during Permian–Triassic time. The Rangnim Massif, the largest Precambrian unit of North Korea, is characterized by a basement that is composed mainly of the upper amphibolite- to granulite-facies Rangnim and Jungsan groups, and overlain by Mesoproterozoic to Phanerozoic sedimentary rocks (Paek *et al.* 1996, p. 619). The Rangnim Group crops out in the northern part of the massif and flanks the margin of the south Phyonngnam Basin, with the main rock types being gneisses, amphibolites, mafic granulites and calc-silicate rocks. The timing of deposition of the meta-sediments in the Rangnim Group has not been well constrained because of the lack of reliable geochronological data. Outcrops of the Jungsan Group are scattered widely in regions to the west of the Phyonngnam Basin and along the western margin of the Rangnim Massif. The group consists of various schists that are characterized by the presence of garnet and sillimanite; the protoliths of these schists were deposited before *c.* 1.9 Ga and underwent

strong metamorphic overprinting and anatexis during the period 1.9–1.8 Ga (Zhao *et al.* 2006, 2016b; Yang *et al.* 2016). Spatially and temporally associated with these so-called supracrustal rocks are voluminous granitoid plutons, including tonalitic–trondhjemitic–granodioritic gneisses and garnet–sillimanite-bearing S-type granites as well as massive porphyritic granites and syenites (Paek *et al.* 1996, p. 619; Zhao *et al.* 2006; Wu *et al.* 2007a; Peng *et al.* 2016). Geochronological studies have shown that these igneous rocks were formed mainly at 1.9–1.8 Ga but with a small number of 2.6–2.5 Ga ages reported along the southern and eastern margins of the Rangnim Massif (Zhao *et al.* 2006, 2016a; Wu *et al.* 2007b; Peng *et al.* 2016; Zhang *et al.* 2016). Mesozoic magmatic rocks are distributed widely within the Rangnim Massif and include Triassic (247–213 Ma) granites, syenites, dolerites and kimberlites, Jurassic (197–163 Ma) granites and Cretaceous (118–106 Ma) granites (Wu *et al.* 2007a; Zhai *et al.* 2016).

Most of the Mesoproterozoic–Phanerozoic sedimentary cover rocks are distributed in the Phyongnam Basin where they are deposited unconformably on the southern basement of the Rangnim Massif. The Phyongnam Basin contains a thick sequence of greenschist-facies metasedimentary rocks. The Sangwon System (Jikhyon, Sadangu, Mukchon and Myoraksan series) at the bottom of this sequence is distributed widely in the central part of the basin, and consists of a thick (*c.* 7000 m) succession of conglomerates, quartzites, phyllites, dolomites, limestones and marble. Hu *et al.* (2012) suggested that the age of deposition of the Sangwon metasediments is no older than 984 Ma. The Kuhyon System (Pirangdong and Rungri series) at the top of the sequence of metasediments in the Phyongnam Basin was deposited unconformably on the Sangwon System of rocks, and comprises conglomerates, phyllites, shales, dolomites and siltstones. A few mafic sills and dykes that have provided a baddeleyite Pb–Pb age of 899 ± 7 Ma were intruded into the rocks of the Sangwon System but were overlain by the sediments of the Kuhyon System (Peng *et al.* 2011), indicating that the Sangwon System was deposited at *c.* 900 Ma. The uppermost Phanerozoic strata belong mainly to the Hwagju System, which consists of Cambrian–Silurian terrigenous clastic rocks and carbonate rocks.

The kimberlites of North Korea are distributed within the Phyongnam Basin, where they appear as dykes and pipes that were intruded into the Jikhyon Series and the Precambrian basement (Fig. 1c). The rocks of the Jikhyon Series constitute the lowermost strata of the Sangwon System and unconformably overlie the Precambrian basement. They consist mainly of conglomerates, quartzites, chlorite schists and pelitic limestones, and contamination from these rocks may have altered the composition of the kimberlitic magma. Most of the kimberlites are porphyritic and have undergone high levels of surface alteration. The phenocrysts of olivine (pseudomorphs), phlogopite and pyroxene are set in a groundmass of mica, serpentine, ilmenite, pyroxene and carbonate. Mantle and/or crustal xenoliths, as well as xenocrysts and phenocrysts, are common in the kimberlites. Phlogopite phenocrysts from these rocks have yielded an Rb–Sr isochron age of 223 ± 7 Ma (Yang *et al.* 2010), which represents the time of kimberlite crystallization. The mantle xenoliths captured by the kimberlites are mainly spinel peridotites, and garnet-bearing peridotites are absent. Previous research (Yang *et al.* 2010) has indicated that these kimberlites have geochemical features similar to those of the Group II kimberlites of Smith (1983). The parental magmas of these kimberlites were formed by a small degree of partial melting of ancient lithospheric mantle at depths where garnet was stable (Yang *et al.* 2010).

3. Analytical methods

The *in situ* U–Pb dating of the zircons was performed using laser ablation inductively coupled plasma mass spectrometry (LA-ICP-MS), whereas the Hf isotope analyses of the zircons were performed using LA multi-collector (MC) ICP-MS. All the analytical work was performed at the Institute of Geology and Geophysics, Chinese Academy of Sciences (IGGCAS).

3.a. Zircon LA-ICP-MS U–Pb dating and trace-element analyses

Fresh samples were crushed and the heavy mineral fractions, including zircon, were extracted using standard techniques. Zircon grains were handpicked under a binocular microscope, mounted in epoxy resin and polished until the grain centres were exposed. Cathodoluminescence (CL) images of the zircons were obtained with a LEO1450VP scanning electron microscope, and the images were used to characterize internal structures and to choose potential target sites for the U–Pb dating and Hf isotope analyses. The acceleration voltage during the CL imaging was 15 kV.

Laser ablation ICP-MS U–Pb analyses of the zircons were conducted using an Agilent 7500a ICP-MS instrument equipped with a 193 nm laser. The frequency for the analyses was 5 Hz, and the spot size for the laser was 32–44 μm . A total of 30–60 analyses per sample were performed for age determinations, with every 10 unknowns being bracketed by two standard zircons 91500 and one reference zircon GJ-1. Zircon 91500 was used as the external calibration standard, whereas zircon GJ-1 was treated as an unknown and used as an independent control on reproducibility and instrument stability. The standard silicate glass NIST 610 was used to optimize the instrument. Common Pb was not subtracted because of the large uncertainty in the determination of ^{204}Pb , as noted elsewhere (Belousova *et al.* 2001; Andersen, 2002; Jackson *et al.* 2004). Raw count rates for ^{29}Si , ^{204}Pb , ^{206}Pb , ^{207}Pb , ^{208}Pb , ^{232}Th and ^{238}U were collected for age determinations. Trace-element concentrations were calibrated using ^{29}Si for internal calibration and NIST 610 as the calibration standard. $^{207}\text{Pb}/^{206}\text{Pb}$ and $^{206}\text{Pb}/^{238}\text{U}$ ratios were calculated using the GLITTER programme. As outlined in Ballard *et al.* (2001), measured $^{207}\text{Pb}/^{206}\text{Pb}$, $^{206}\text{Pb}/^{238}\text{U}$ and $^{208}\text{Pb}/^{232}\text{Th}$ ratios in zircon 91500 were averaged over the course of an analytical session and used to calculate correction factors. These correction factors were then applied to each sample to correct for both instrumental mass bias and depth-dependent elemental and isotopic fractionation. The age calculations and concordia plots were constructed using ISOPLOT (v. 3.0) (Ludwig, 2003).

3.b. LA-MC-ICP-MS zircon Hf isotope analyses

Zircon Hf isotope analyses were conducted using a Neptune MC-ICP-MS instrument with an attached 193 nm excimer ArF laser ablation system. Lu–Hf isotope measurements were made on the same zircon grains that had been used for U–Pb dating. During Hf analyses, a laser repetition rate of 8 Hz and 15 J cm^{-2} was used, and the spot size was 60 μm . Raw count rates for ^{172}Yb , ^{173}Yb , ^{175}Lu , $^{176}(\text{Hf} + \text{Yb} + \text{Lu})$, ^{177}Hf , ^{178}Hf , ^{179}Hf , ^{180}Hf and ^{182}W were collected, and isobaric interference corrections for ^{176}Lu and ^{176}Yb on ^{176}Hf were determined precisely. The analytical procedures and the corrections for interferences have been described by Wu *et al.* (2006). During the analyses, the $^{176}\text{Hf}/^{177}\text{Hf}$ ratios determined for the standard zircon Mud Tank were 0.282499 ± 5 ($2\sigma_n$, $n = 34$), similar to the commonly accepted $^{176}\text{Hf}/^{177}\text{Hf}$ ratio of 0.282507 ± 6

measured using the solution method (Woodhead *et al.* 2004). The $^{176}\text{Hf}/^{177}\text{Hf}$ ratio determined for the standard zircon GJ-1 was 0.282008 ± 6 ($2\sigma_n$, $n = 28$), which is similar to the commonly accepted $^{176}\text{Hf}/^{177}\text{Hf}$ ratio of 0.282015 ± 19 ($2\sigma_n$, $n = 25$) (Elhlou *et al.* 2006).

4. Results

4.a. U–Pb ages and trace elements

A total of 140 analyses were obtained on 138 zircon grains from six kimberlite samples (11NK11, 11NK12, 11NK13, 11NK14, T-1 and T-2). The U–Pb results and rare Earth element (REE) concentrations are listed in the online Supplementary Tables S1 and S2 (available at <http://journals.cambridge.org/geo>). CL images of representative zircons are shown in Figure 2a. Most zircon grains are euhedral to subhedral with sizes of 50–120 μm , and exhibit stubby prismatic or ellipsoidal morphologies. The majority of zircons display fine-scale oscillatory growth zoning (Fig. 2a), which is a typical characteristic of magmatic zircon (Corfu *et al.* 2003). These zircons have variable Th (28–511 ppm) and U (91–905 ppm) contents with Th/U ratios (mostly 0.11–1.05) that are higher than the typical 0.1 of metamorphic zircons (Rubatto, 2002) (online Supplementary Table S1). The chondrite-normalized REE diagram (Fig. 2b) shows that the zircons are characterized by enrichment in heavy REEs, depletion of light REEs and marked positive Ce and negative Eu anomalies (Fig. 2b and online Supplementary Table S2). These features suggest that most of the zircons analysed for this study were magmatic in origin (Hoskin & Black, 2000; Belousova *et al.* 2002).

No reliable Archaean zircon ages were identified during our work (online Supplementary Table S1), and the oldest ages are Palaeoproterozoic (Fig. 3 and online Supplementary Table S1). Four analyses yielded the oldest $^{207}\text{Pb}/^{206}\text{Pb}$ ages, which range from 2402 ± 11 to 2442 ± 12 Ma, with a weighted mean $^{207}\text{Pb}/^{206}\text{Pb}$ age of 2419 ± 29 Ma (2σ , mean square weighted deviation (MSWD) = 2.3). Three concordant analyses gave ages of 1999 ± 15 , 2151 ± 22 and 2246 ± 16 Ma. However, most of our 128 analyses gave ages of 1.9–1.8 Ga with a weighted mean $^{207}\text{Pb}/^{206}\text{Pb}$ age of 1879 ± 3 Ma (2σ , MSWD = 1.4) (Fig. 3). Two late Palaeoproterozoic–Mesoproterozoic zircons appear in our data, with one yielding a $^{207}\text{Pb}/^{206}\text{Pb}$ age of 1694 ± 51 Ma and the other a $^{207}\text{Pb}/^{206}\text{Pb}$ age of 1184 ± 18 Ma. The remaining three zircon grains are Phanerozoic and have a weighted mean $^{206}\text{Pb}/^{238}\text{U}$ age of 463 ± 8 Ma (2σ , MSWD = 0.1) (Fig. 3). A histogram for zircons of this study is shown in Figure 4a. Given that at least three grains are required to define an age population, the zircon ages show one prominent age peak at 1.8–1.9 Ga and two weak age peaks at c. 460 Ma and c. 2.4 Ga.

4.b. Results of the zircon Hf isotope analyses

The measurements of Hf isotopes were made on the same zircon grains that had been used for U–Pb dating and mostly reoccupying the previous U–Pb analytical spots. The Hf data are listed in the online Supplementary Table S3 (available at <http://journals.cambridge.org/geo>).

The zircons we analysed for this study exhibit a wide range of $^{176}\text{Lu}/^{177}\text{Hf}$ ratios (0.0003–0.0018). Comparatively, the Precambrian zircon grains (c. 2.4–1.7 Ga) have less radiogenic $^{176}\text{Hf}/^{177}\text{Hf}$ ratios (0.280996–0.282092) than those with Phanerozoic ages (0.282389–0.282932), and they yield low $\epsilon_{\text{Hf}}(t)$ values of -9.7 to $+0.7$, corresponding to the Hf model ages (T_{DM}^{C}) of 2.6–3.6 Ga (online Supplementary Table S3). In Figure 5, the data plot along the average

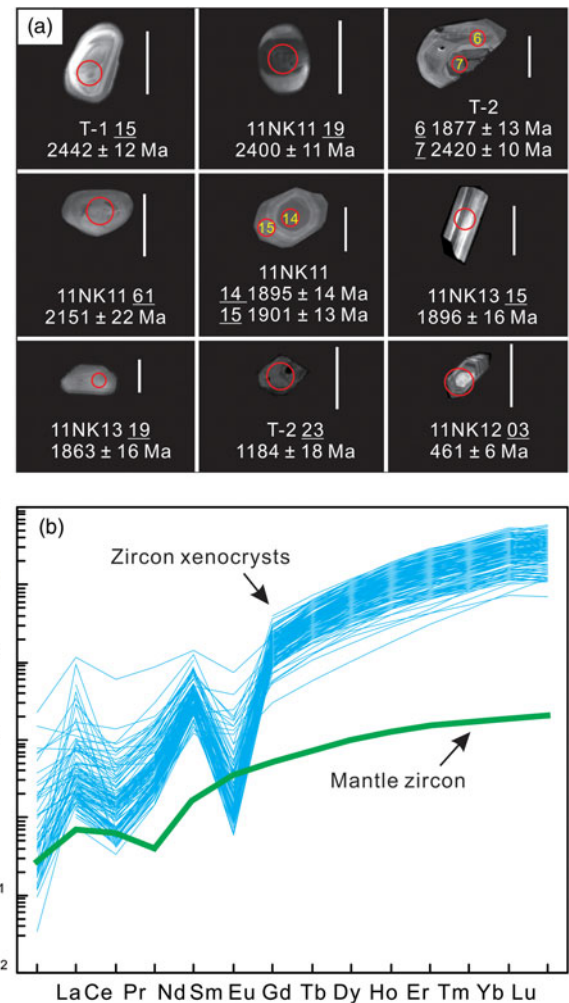


Fig. 2. (Colour online) (a) Cathodoluminescence images of representative dated zircon xenocrysts from kimberlite samples of North Korea (the length of the scale bar is 100 μm). (b) Chondrite-normalized REE distribution diagram of the zircon xenocrysts from the North Korean kimberlites showing comparisons with the mantle zircons of Belousova *et al.* (1998). The chondrite values are from Sun & McDonough (1989).

continental crust evolution trend. The zircon with a Mesoproterozoic age has a weakly positive $\epsilon_{\text{Hf}}(t)$ value (+1.5), corresponding to a Hf model age of 1.9 Ga. The Phanerozoic zircons (c. 460 Ma) display much higher $\epsilon_{\text{Hf}}(t)$ values (-3.5 to $+15.3$) (online Supplementary Table S3) and plot close to the depleted mantle evolution line on Figure 5. The Hf model ages of these Phanerozoic zircons ($T_{\text{DM}}^{\text{C}} = 1665\text{--}466$ Ma) are similar or close to the zircon crystallization ages and are significantly different from those of the Precambrian zircons (online Supplementary Table S3).

5. Discussion

5.a. The origin of zircon xenocrysts in the kimberlites

Because of the low silica contents of kimberlitic magmas and their relatively high alkali contents and high temperatures, it is difficult for kimberlitic magmas to crystallize primary phenocrysts of zircon (Krasnobayev, 1980; Belousova *et al.* 1998; Griffin *et al.* 1999; Robles-Cruz *et al.* 2012; Donatti-Filho *et al.* 2013), and most zircons in kimberlites are captured from the mantle or crustal wall rocks during magma ascent (Krasnobayev, 1980; Robles-Cruz *et al.* 2012; Donatti-Filho *et al.* 2013). In other words, the crystallization

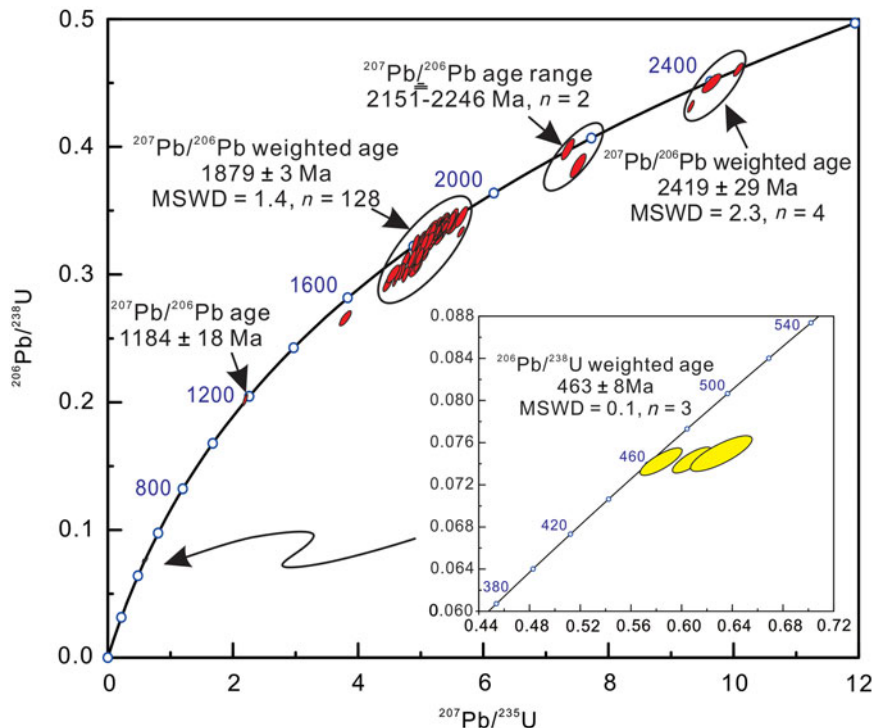


Fig. 3. (Colour online) U–Pb concordia diagram for the zircon xenocrysts from our five kimberlite samples.

of these zircons is related to geological processes that took place prior to the kimberlitic magmatism (Allsopp *et al.* 1989; Valley *et al.* 1998; Griffin *et al.* 2000; Belousova *et al.* 2001; Zheng *et al.* 2009). The zircons that we separated from the North Korean kimberlites show ages that range from *c.* 2.4 to 0.46 Ga (online Supplementary Table S1), which are significantly older than the age of formation of the host kimberlite (223 ± 7 Ma, Yang *et al.* 2010), and these zircons therefore represent mantle or crustal xenocrysts captured by the host kimberlitic magma.

Inferences as to the sources of zircon xenocrysts in kimberlites can be made from their crystal morphology and trace-element contents (Kresten *et al.* 1975; Krasnobayev, 1980; Mitchell, 1986; Belousova, Griffin & Pearson, 1998; Belousova *et al.* 2002; Robles-Cruz *et al.* 2012; Donatti-Filho, Oliveira & McNaughton, 2013). Mantle zircons usually have a large grain size (typically several millimetres) and display either wide oscillatory zones or a homogeneous structure in CL images (Kresten *et al.* 1975; Krasnobayev, 1980; Belousova *et al.* 1998, 2002; Sun *et al.* 2018). Their uranium and thorium contents are low and rarely exceed 50–60 ppm for U and 10–15 ppm for Th (Belousova *et al.* 1998, 2002). Mantle zircons have REE contents lower than 50 ppm and show weak or no Eu anomalies in chondrite-normalized REE patterns (Fig. 2b) (Belousova *et al.* 1998, 2002). However, zircons in the Triassic kimberlites are characterized by narrow oscillatory zones and a grain size of $< 150 \mu\text{m}$. Most of these kimberlite zircons display markedly negative Eu anomalies, high Th (28–511 ppm) and U (91–915 ppm) abundances and high total REE contents (Figs 2b and 6a). These features suggest that the zircon xenocrysts from the North Korean kimberlites were derived from crustal rather than mantle rocks. Furthermore, the relatively high Y contents and high U/Yb values (Fig. 6b) indicate that these zircon xenocrysts probably had an origin in continental crust rather than being inherited from a recycled oceanic crust characterized by low U/Yb ratios (Grimes *et al.* 2007). The principal provenance for these zircons is therefore likely to have been the Rangnim Massif.

As has been pointed out previously, the host kimberlites were intruded into the rocks of the Jikhyon Series, and these sedimentary rocks may have provided a source for some of the zircon xenocrysts in the North Korean kimberlites (Parrish & Reichenbach, 1991; Batumike *et al.* 2007). However, detrital zircons in sedimentary rocks are in all cases characterized by some degree of rounding, and this characteristic was not observed in the subhedral–euhedral zircon grains that we analysed. More importantly, the *in situ* U–Pb dating of detrital zircons from the Jikhyon Series reveals two distinct age peaks at 1.6–1.4 and 1.2–1.0 Ga and a relatively weak age peak at 1.9–1.8 Ga (Fig. 4b) (Hu *et al.* 2012; Li *et al.* 2016), and this age spectrum differs drastically from that of the zircon xenocrysts from the North Korean kimberlites. It therefore seems likely that these zircon xenocrysts were derived from the underlying crystalline basement rock and that the ages and Hf isotope characteristics of these xenocrysts should help us to establish the nature of the basement beneath the Rangnim Massif.

5.b. Zircon records of a Palaeoproterozoic basement

The kimberlites of North Korea are located in the Phyongnam Basin, which was developed on the southern side of the Rangnim Massif. Because of the widespread and thick Mesoproterozoic to Palaeozoic sedimentary cover rocks, the nature of the basement rocks beneath this region is not well constrained. Recently, Neoproterozoic granitoid rocks with *in situ* zircon U–Pb ages of 2.64–2.52 Ga have been found along the southern and eastern margins of the basin (Zhao *et al.* 2006, 2016a), and these unique Archaean ages are consistent with the prior Archaean isochron dating results of Paek *et al.* (1996, p. 619), implying that more Archaean rocks may exist in the southern part of the Rangnim Massif. The zircon xenocrysts in the kimberlites offer a direct way of investigating the hidden basement of the basin, but the 138 zircon xenocrysts that we analysed revealed no concordant Archaean ages. The oldest

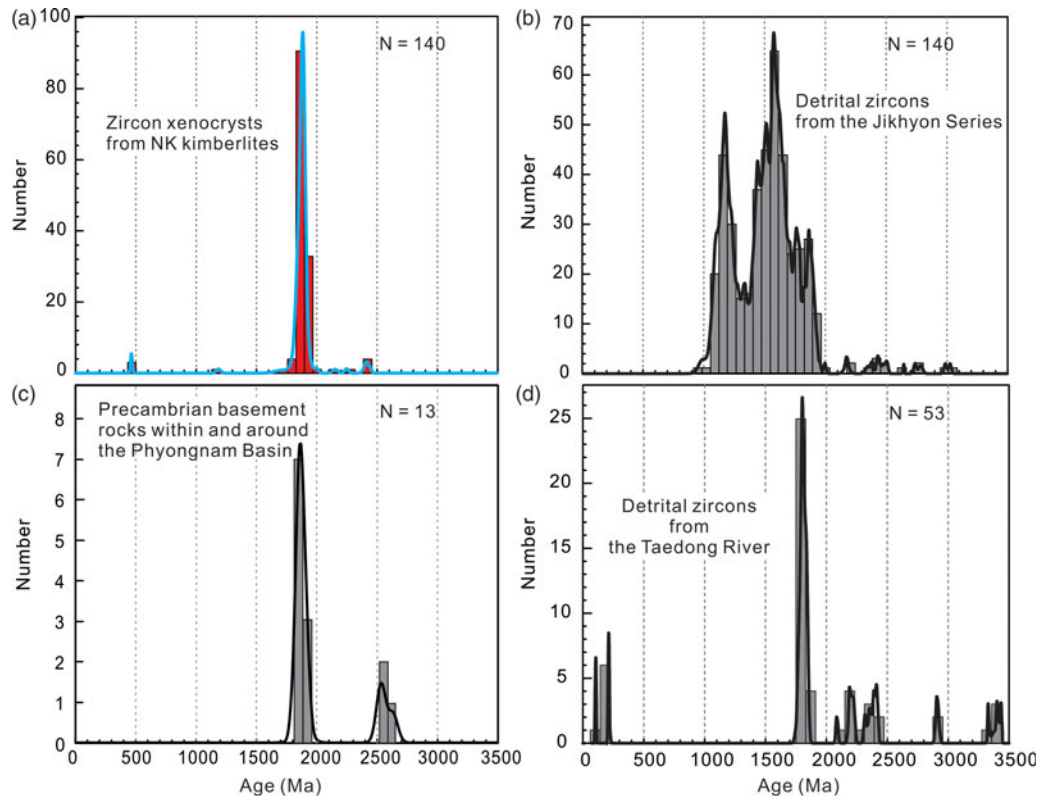


Fig. 4. (Colour online) (a) Probability diagrams of U–Pb ages for zircon xenocrysts from the North Korean kimberlites, (b) detrital zircons from the Jikhyon Series, (c) Precambrian basement rocks within and around the Phyongnam Basin, and (d) detrital zircons from the Taedong River, North Korea. Data for the detrital zircons are from Wu *et al.* (2007b, 2016), and data for the Precambrian basement rocks are from Peng *et al.* (2016).

age population, yielded by just four zircons, is a cluster at *c.* 2.4 Ga (online Supplementary Table S1 and Fig. 4a). These age data therefore suggest that Archaean basement rocks are of very limited extent or absent from beneath the Phyongnam Basin. The recently identified Archaean granitic rocks (Zhao *et al.* 2016a) might be restricted in scale and of limited extent at depth, and may represent remnants of Archaean material that survived the later thermal events (see Section 5.c. below).

The most prominent age population displayed by zircon xenocrysts from the North Korean kimberlites (Fig. 4a) is a cluster at 1.9–1.8 Ga. More than 90% (128 analyses) of the total data are within this range, and they gave a weighted average age of 1879 ± 3 Ma (online Supplementary Table S1). Considering the igneous origin of the xenocryst zircons and their derivation from crustal rocks, we suggest that a thick Palaeoproterozoic-dominant crustal component lies hidden at depth beneath the kimberlite region. This proposition is supported by the Palaeoproterozoic rocks that are widely exposed within and around the Phyongnam Basin (Fig. 4c). These rocks include massive porphyritic monzogranites, biotite granites, garnet–sillimanite granites and syenites with zircon U–Pb ages that range from 1908 ± 12 to 1854 ± 12 Ma (Zhao *et al.* 2006; Wu *et al.* 2007a; Peng *et al.* 2016), and their outcrops indicate that they exist in a much larger volume than the Archaean remnants. Furthermore, Wu *et al.* (2007b) examined detrital zircons collected from sands at the mouth of the Tedong River, which traverses the Phyongnam Basin, as a way of indirectly sampling the Rangnim Massif, and their age data also display a prominent age peak at 1.9–1.8 Ga (Fig. 4d).

In summary, the exposed basement rocks surrounding the Phyongnam Basin are predominantly of Palaeoproterozoic age, and their ages are consistent with the Palaeoproterozoic ages of

the zircon xenocrysts that were derived from the hidden crustal components beneath the basin. The data therefore indicate that a widespread Palaeoproterozoic basement exists in the southern part of the Rangnim Massif.

The northern part of the Rangnim Massif has been considered to be a region with major outcrops of Precambrian basement rock (Paek *et al.* 1996, p. 619). However, fieldtrips and rock sampling are not possible in this region. As an alternative strategy, Wu *et al.* (2007b) obtained samples from the major rivers that traverse the northern part of the Rangnim Massif, namely the Songchon and Chongchon rivers. The U–Pb ages of zircons collected from the mouths of these rivers feature a prominent age peak at 1.9–1.8 Ga, along with a few Archaean ages. Furthermore, among the few geochronological data reported for the rocks exposed in this region, no reliable dates for Archaean intrusions have been found (Zhao *et al.* 2006; Wu *et al.* 2007a; Zhai *et al.* 2007a). Moreover, Archaean ages are also lacking in the adjacent region of China that was thought to be connected geologically with the Rangnim Massif of North Korea (Wang *et al.* 2015). The majority of Precambrian rocks in the northern part of the Rangnim Massif are therefore probably of Palaeoproterozoic age, consistent with the southern part of the massif. We therefore suggest that, during Triassic time when the kimberlites were emplaced, the basement component of the Rangnim Massif was dominated by Palaeoproterozoic rocks. Although Archaean components are exposed locally at the surface, there is no evidence that they are widespread at depth.

The weak age population at 463 ± 8 Ma (Fig. 4a) has seldom been reported in North Korea, and it is significantly older than the *c.* 400 Ma metamorphic event recorded by the Neoproterozoic mafic dykes in the Phyongnam Basin (Peng *et al.* 2011), thus precluding any relationship with that event. In the adjacent eastern NCC,

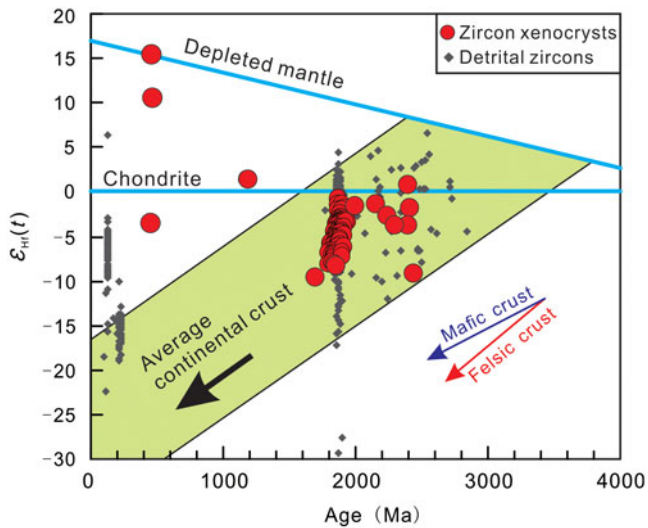


Fig. 5. (Colour online) Temporal variations in Hf values of the studied zircon xenocrysts. The black diamond shapes represent detrital zircons from North Korean rivers (Wu *et al.* 2007b).

Ordovician diamondiferous kimberlites were emplaced at 480 ± 4 Ma (Li *et al.* 2011), and they represent the only known magmatism of Palaeozoic age within the craton. It is therefore possible that a similar magmatic event might also have occurred in North Korea, but slightly earlier than that in the NCC. However, the information on these events is very scarce, and further work is needed to ascertain the geological significance of these Palaeozoic zircons.

5.c. A Palaeoproterozoic crustal reworking event recorded by zircon xenocrysts

Although the Archaean materials are much more limited in scale than the Palaeoproterozoic rocks, their footprints can be traced widely in the Rangnim Massif. In addition to the exposed Archaean rocks mentioned above, inherited zircons of Archaean age have been found in North Korea in the Palaeoproterozoic granitic gneisses and in the sediments of modern rivers, and some of these zircons are as old as 3.2 Ga (Zhao *et al.* 2006; Wu *et al.* 2007a, b; Zhai *et al.* 2007a). The question arises, therefore, as to whether the dominant Palaeoproterozoic basement rocks of the Rangnim Massif were derived from the reworking of those Archaean rocks or whether they simply represent a strong crustal growth event.

Zircon can provide information on the Hf isotope composition of the magma from which it crystallized (Cherniak *et al.* 1997a, b; Kinny & Maas, 2003). Accordingly, Hf isotope data can be used to determine whether a zircon crystallized from a juvenile source or whether it was the result of ancient crustal recycling. Our Hf isotope analyses revealed that the zircons with Palaeoproterozoic ages have lowly radiogenic Hf isotopes with $\epsilon_{\text{Hf}}(t)$ values of -9.7 to $+0.7$, and all these values are much lower than those of depleted mantle (Fig. 5), indicating that these zircons were not juvenile but derived from the recycling of more ancient crust. Statistical calculations indicate that these Palaeoproterozoic zircons have an average Hf model age of 2.86 ± 0.02 Ga (2σ) (Fig. 7a), identical to the Hf model age of 2.89 ± 0.03 Ga (2σ) given by Precambrian detrital zircons from the river sands of North Korea (Wu *et al.* 2007b). These features indicate that much older crustal components existed in the Rangnim Massif before the Palaeoproterozoic Era.

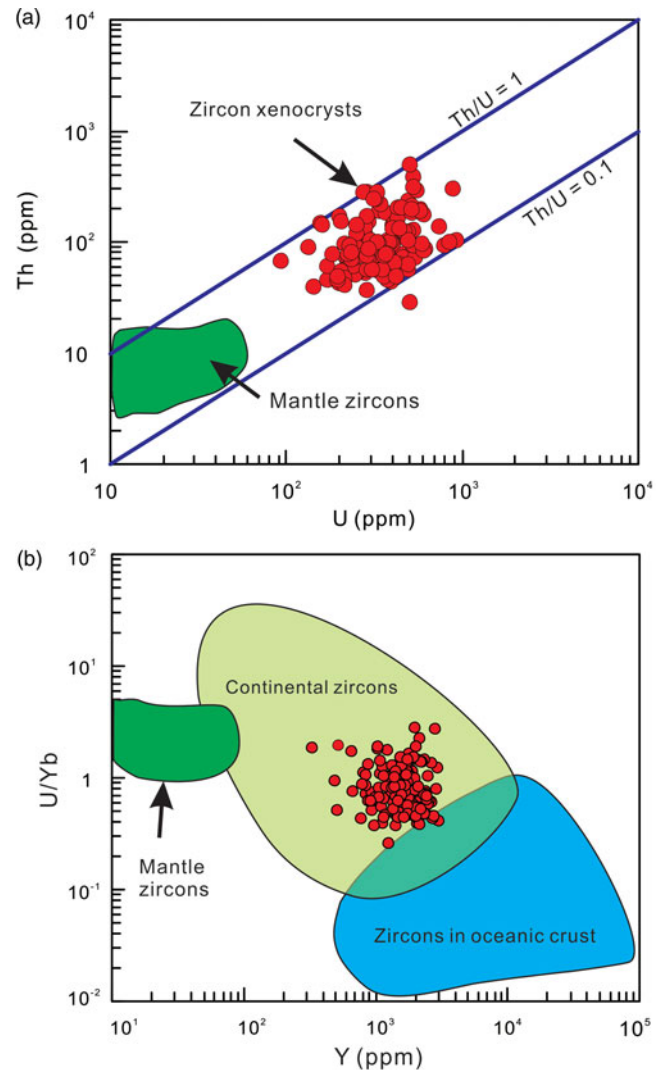


Fig. 6. (Colour online) Diagrams of (a) Th v. U and (b) U/Yb v. Y (Grimes *et al.* 2007) showing the origins of the zircons. The data for mantle zircons in kimberlites are from Donatti-Filho *et al.* (2013).

A few Archaean zircons have been found in river sands collected from the mouths of North Korean rivers (Wu *et al.* 2007b), although zircons of such ages are not present in our samples. Most of the Archaean zircons of Wu *et al.* (2007b) have $\epsilon_{\text{Hf}}(t)$ values of -0.7 to $+6.5$, therefore falling between the evolutionary trend of depleted mantle and chondrite in Figure 5. These characteristics indicate that the protoliths of those Archaean zircons were juvenile during the Archaean Eon and that they possibly represent the initial crust of the Rangnim Massif. However, our work shows that those Archaean components have barely survived since the Triassic Period. Considering the wide distribution of 1.9–1.8 Ga basement rocks beneath the Rangnim Massif and their generation as a result of the re-melting of ancient crust, we suggest that a strong crustal reworking event occurred in the Rangnim Massif during the Palaeoproterozoic Era. Large volumes of crust- and mantle-derived magmatic rocks were generated repeatedly in the massif during this time, and those processes continuously digested the pre-existing basement, thus exhausting most of the supply of Archaean rock. Only scarce remnants of Archaean material survived to be sparsely distributed within the newly formed Palaeoproterozoic basement.

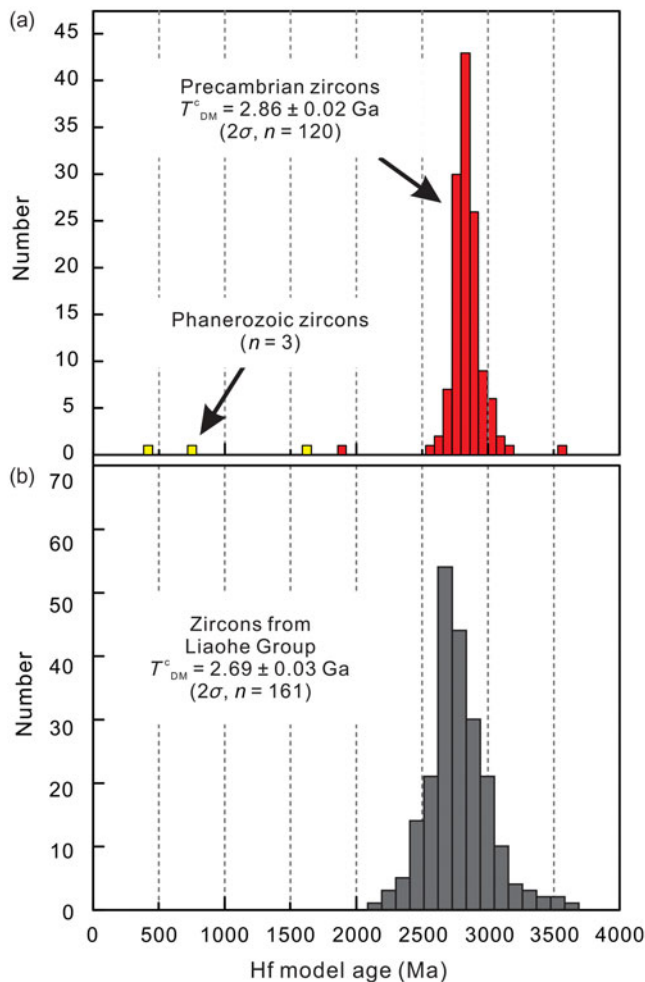


Fig. 7. (Colour online) Histograms showing the Hf model ages (a) of zircon xenocrysts from the North Korean kimberlites and (b) of detrital zircons from the Liaohe Group within the Liao–Ji Belt. Data for the Liaohe Group are from Luo *et al.* (2008).

5.d. Implications for the tectonic affinity of the Rangnim Massif

It has been widely accepted that the basement of the Rangnim Massif is connected to that of the NCC (Cluzel *et al.* 1991; Yin & Nie, 1993; Ernst & Liou, 1995; Chang, 1996; Chang & Park, 2001; Kim *et al.* 2006; Metcalfe, 2006; Oh, 2006; Zhao *et al.* 2006; Wu *et al.* 2007b; Zhai *et al.* 2007b, c; Oh *et al.* 2015), and that both terranes underwent similar geological evolutions during Phanerozoic time. However, the northeastern part of the NCC is composed of the Archaean Liaobei and Liaonan blocks and the intervening Palaeoproterozoic Liao–Ji mobile belt (Fig. 1b). These tectonic units record a distinctive Precambrian geological history (Zhao *et al.* 2001, 2005); the key to constraining the tectonic affinity of the Rangnim Massif therefore lies in making comparisons between the Rangnim Massif and these tectonic units. The Rangnim Massif was once thought to contain widespread areas of Archaean rock and was therefore treated as the eastern extension of the Archaean Liaonan Block (Bai, 1993; Zhao *et al.* 1998, 2005; Zhao & Zhai, 2013), with the Archaean Liaonan–Rangnim Massif representing one of the most ancient continental nuclei in the NCC. However, our work and that of others over the past 10 years has revealed that Archaean rocks are actually very scarce within the Rangnim Massif. This means that the massif differs significantly


from the Liaonan Block, as the Liaonan Block has extensive exposure of late Archaean TTG rocks, and this in turn makes comparative studies of the Rangnim Massif and Liaonan Block difficult.

The Rangnim Massif is characterized by 1.9–1.8 Ga magmatic activity. This thermal event has also been well documented in the Liao–Ji mobile belt (Faure *et al.* 2004; Luo *et al.* 2004; Lu *et al.* 2006; Li & Zhao, 2007; Yang *et al.* 2007). The belt consists of the supracrustal rocks of the Liaohe Group (and equivalent assemblages in Jilin Province) (LBGMR, 1989) and voluminous Palaeoproterozoic granitic rocks. The sediments of the Liaohe Group were deposited between the Archaean Liaobei and Liaonan blocks and were metamorphosed at 1.93 Ga (Luo *et al.* 2004; Xie *et al.* 2011). The associated granitoids can be divided into 2.17–2.09 and 1.88–1.85 Ga granites (Lu *et al.* 2006; Li & Zhao, 2007; Yang *et al.* 2007), and the younger of these granitic suites contains garnet- and cordierite-bearing porphyritic S-type granite, hornblende-bearing quartz diorite, porphyritic granodiorite and syenite. The granites are similar to the 1.9–1.8 Ga Ryonhwasan S-type granites, the Myohyangsan porphyritic granites and the Sakju syenites, all of which are present in the Rangnim Massif (Zhao *et al.* 2005; Wu *et al.* 2007a; Zhai *et al.* 2007a; Kim *et al.* 2016; Peng *et al.* 2016). In addition, detrital zircons from the Liaohe Group sediments have provenances dominated by the Palaeoproterozoic Liao–Ji granitoids along with small amounts of late Archaean basement rocks. The Liaohe Group zircons have an average Hf model age of 2.69 ± 0.03 Ga (Fig. 7b) (Luo *et al.* 2008), and this is comparable to the model ages of our samples of zircon xenocrysts from the Rangnim Massif, thus indicating the coeval formation of continental crust in both areas. These observations suggest that the Rangnim Massif is more likely to be part of the Liao–Ji mobile belt (Peng *et al.* 2011, 2016; Liu *et al.* 2015; Wang *et al.* 2015; Wu *et al.* 2016) than of Archaean Liaonan Block. The Liao–Ji Belt is one of the Palaeoproterozoic orogens within the NCC and was previously considered to have been formed during the amalgamation of the Archaean Liaobei–Longgang Block and the Archaean Liaonan–Rangnim Block, thus marking the final stage in the formation of the NCC (Zhao *et al.* 2001, 2005). However, if the Rangnim Massif were part of the Liao–Ji Belt, then this would indicate the presence of a huge Palaeoproterozoic orogen in the eastern NCC. If this were the case, then a complete reappraisal of the Precambrian evolution of the eastern Sino-Korean Craton would be needed to understand the geodynamic evolution of this huge orogen and its role in the evolution of the NCC.

6. Conclusions

- (1) Zircons in the North Korean Triassic kimberlites are xenocrysts that were captured from the deep crust during magma ascent.
- (2) Most of the zircon xenocrysts are of igneous origin and crystallized at 1.9–1.8 Ga. Zircons of Archaean age were not found. The age spectrum for the zircons clearly indicates a Palaeoproterozoic provenance, which implies the presence of a Palaeoproterozoic basement beneath the Rangnim Massif.
- (3) The Hf isotope data reveal that the Rangnim Massif once had an Archaean basement. During the Palaeoproterozoic Era, a strong crustal reworking event significantly modified the pre-existing Archaean crust of the Rangnim Massif and generated a basement that was dominated by Palaeoproterozoic materials.
- (4) The Rangnim Massif shows a greater tectonic affinity with the Palaeoproterozoic Liao–Ji Belt of the NCC than with the

Archaean Liaonan Block, and this poses significant problems for previous ideas on geological relationships in the Sino-Korean area. Our new data indicate the presence of a huge Palaeoproterozoic orogen in the eastern NCC, and the geological evolution of this area now requires a complete reappraisal.

Author ORCIDs.  Yu-Sheng Zhu 0000-0002-1121-2506

Acknowledgements. We thank Yue-Heng Yang and Lie-Wen Xie for their help in determining the U–Pb ages and Hf isotope contents of the zircons. We also thank Peng Peng for discussions on the geology of kimberlites in North Korea. We are grateful to two anonymous reviewers for their thoughtful and constructive comments and to the editor for handling this paper. This study was supported by funds from the Ministry of Science and Technology of the People's Republic of China (2016YFC0600109), the National Natural Science Foundation of China (41702059) and the China Postdoctoral Science Foundation.

Supplementary material. To view supplementary material for this article, please visit <https://doi.org/10.1017/S0016756818000900>.

Declaration of interest. None.

References

- Allsopp HL, Bristow JW, Smith CB, Brown R, Gleadow AJW, Kramers JD and Garvie OG (1989) A summary of radiometric dating methods applicable to kimberlite and related rocks. In *Kimberlite and Related Rocks: Their Composition, Occurrence, Origin and Emplacement* (ed. JL Ross), pp. 343–57. Oxford: Blackwell Scientific Publications.
- Andersen T (2002) Correction of common lead in U–Pb analyses that do not report ²⁰⁴Pb. *Chemical Geology* **192**, 59–79.
- Ashchepkov IV, Rotman AY, Somov SV, Afanasiev VP, Downes H, Logvinova AM, Nossyko S, Shimupi J, Palesky SV, Khmelnikova OS and Vladyskin NV (2012) Composition and thermal structure of the lithospheric mantle beneath kimberlite pipes from the Catoca cluster, Angola. *Tectonophysics* **530–1**, 128–51.
- Bai J (1993) *The Precambrian Geology and Pb–Zn Mineralization in the Northern Margin of North China Platform*. Beijing: Geological Publishing House.
- Ballard JR, Palin JM, Williams IS, Campbell IH and Faunes A (2001) Two ages of porphyry intrusion resolved for the super-giant Chuquicamata copper deposit of northern Chile by ELA-ICP-MS and SHRIMP. *Geology* **29**, 383–6.
- Batumike JM, O'Reilly SY, Griffin WL and Belousova EA (2007) U–Pb and Hf-isotope analyses of zircon from the Kundelungu Kimberlites, D.R. Congo: implications for crustal evolution. *Precambrian Research* **156**, 195–225.
- Belousova EA, Griffin WL, O'Reilly SY and Fisher NI (2002) Igneous zircon: trace element composition as an indicator of source rock type. *Contributions to Mineralogy and Petrology* **143**, 602–22.
- Belousova EA, Griffin WL and Pearson NJ (1998) Trace element composition and cathodoluminescence properties of southern African kimberlitic zircons. *Mineralogical Magazine* **62**, 355–66.
- Belousova EA, Griffin WL, Shee SR, Jackson SE and O'Reilly SY (2001) Two age populations of zircons from the Timber Creek kimberlites, Northern Territory, as determined by laser-ablation ICP-MS analysis. *Australian Journal of Earth Sciences* **48**, 757–65.
- Chang EZ (1996) Collisional orogene between north and south China and its eastern extension in the Korean Peninsula. *Journal of Southeast Asian Earth Sciences* **13**, 267–77.
- Chang KH and Park SO (2001) Paleozoic Yellow Sea transform fault: its role in the tectonic history of Korea and adjacent regions. *Gondwana Research* **4**, 588–9.
- Cherniak DJ, Hanchar JM and Watson EB (1997a) Diffusion of tetravalent cations in zircon. *Contributions to Mineralogy and Petrology* **127**, 383–90.
- Cherniak DJ, Hanchar JM and Watson EB (1997b) Rare-earth diffusion in zircon. *Chemical Geology* **134**, 289–301.
- Cluzel D, Lee BJ and Cadet JP (1991) Indosinian dextral ductile fault system and synkinematic plutonism in the southwest of the Ogcheon belt (South Korea). *Tectonophysics* **194**, 131–51.
- Corfu F, Hanchar JMHoskin PWO and Kinny P (2003) Atlas of zircon textures. *Reviews in Mineralogy and Geochemistry* **53**, 469–500.
- Donatti-Filho JP, Oliveira EP and McNaughton NJ (2013) Provenance of zircon xenocrysts in the Neoproterozoic Brauna Kimberlite Field, São Francisco Craton, Brazil: evidence for a thick Palaeoproterozoic lithosphere beneath the Serrinha block. *Journal of South American Earth Sciences* **45**, 83–96.
- Ehrlou S, Belousova E, Griffin WL, Pearson NJ and O'Reilly SY (2006) Trace element and isotopic composition of GJ-red zircon standard by laser ablation. *Geochimica et Cosmochimica Acta* **70**, A158.
- Ernst WG and Liou JG (1995) Contrasting plate-tectonic styles of the Qinling-Dabie-Sulu and Franciscan metamorphic belts. *Geology* **23**, 353–6.
- Faure M, Lin W, Monié P and Bruguier O (2004) Palaeoproterozoic arc magmatism and collision in Liaodong Peninsula (north-east China). *Terra Nova* **16**, 75–80.
- Griffin WL, O'Reilly SY and Ryan CG (1999) The composition and origin of sub-continental lithospheric mantle. In *Mantle Petrology: Field Observations and High-pressure Experimentation: A tribute to Francis R. (Joe) Boyd* (eds Y Fei, CM Bertka and BO Mysen), pp. 13–45. Houston: The Geochemical Society, Special Publication 6.
- Griffin WL, Pearson NJ, Belousova E, Jackson SE, Van Achtenbergh E, O'Reilly SY and Shee SR (2000) The Hf isotope composition of cratonic mantle: LAM-MC-ICPMS analysis of zircon megacrysts in kimberlites. *Geochimica et Cosmochimica Acta* **64**, 133–47.
- Grimes CB, John BE, Kelemen PB, Mazdab FK, Wooden JL, Cheadle MJ, Hangoj K and Schwartz JJ (2007) Trace element chemistry of zircons from oceanic crust: a method for distinguishing detrital zircon provenance. *Geology* **35**, 643–6.
- Hoskin PWO and Black LP (2000) Metamorphic zircon formation by solid-state recrystallization of protolith igneous zircon. *Journal of Metamorphic Geology* **18**, 423–39.
- Hu B, Zhai M, Li T, Li Z, Peng P, Guo J and Kusky TM (2012) Mesoproterozoic magmatic events in the eastern North China Craton and their tectonic implications: geochronological evidence from detrital zircons in the Shandong Peninsula and North Korea. *Gondwana Research* **22**, 828–42.
- Huang JQ (1977) Basic outline of China tectonics. *Acta Geologica Sinica* **52**, 117–35 (in Chinese).
- Jackson SE, Pearson NJ, Griffin WL and Belousova EA (2004) The application of laser ablation-inductively coupled plasma-mass spectrometry to in situ U–Pb zircon geochronology. *Chemical Geology* **211**, 47–69.
- Kelley SP and Wartho JA (2000) Rapid kimberlite ascent and the significance of Ar–Ar ages in xenolith phlogopites. *Science* **289**, 609–11.
- Kemp AIS, Hawkesworth CJ, Paterson BA and Kinny PD (2006) Episodic growth of the Gondwana supercontinent from hafnium and oxygen isotopes in zircon. *Nature* **439**, 580–83.
- Kim JN, Han RY, Zhao L, Li QL and Kim S (2016) Study on the petrographic and SIMS zircon U–Pb geochronological characteristics of the magmatic rocks and associated with the Jongju and Cholsan REE deposits in northern Korean Peninsula. *Acta Petrologica Sinica* **32**, 3123–38 (in Chinese with English abstract).
- Kim SW, Oh CW, Williams IS, Rubatto D, Ryu I-C, Rajesh VJ, Kim CB, Guo J and Zhai M (2006) Phanerozoic high-pressure eclogite and intermediate-pressure granulite facies metamorphism in the Gyeonggi Massif, South Korea: implications for the eastward extension of the Dabie–Sulu continental collision zone. *Lithos* **92**, 357–77.
- Kinny PD and Maas R (2003) Lu–Hf and Sm–Nd isotope systems in zircon. In *Zircon* (eds JM Hanchar and PWO Hoskin), pp. 327–39. Washington: Reviews in Mineralogy and Geochemistry.
- Kostrovitsky SI, Skuzovatov SY, Yakovlev DA, Sun J, Nasdala L and Wu F-Y (2016) Age of the Siberian craton crust beneath the northern kimberlite fields: insights to the craton evolution. *Gondwana Research* **39**, 365–85.
- Krasnobayev AA (1980) Mineralogical-geochemical features of zircons from kimberlites and problems of their origin. *International Geology Review* **22**, 1199–209.

- Kresten P, Fels P and Berggren G** (1975) Kimberlitic zircons — A possible aid in prospecting for kimberlites. *Mineralium Deposita* **10**, 47–56.
- Kwon S, Sajeev K, Mitra G, Park Y, Kim SW and Ryu IC** (2009) Evidence for Permo-Triassic collision in Far East Asia: the Korean collisional orogen. *Earth and Planetary Science Letters* **279**, 340–9.
- LBGMR (Liaoning Bureau of Geology and Mineral Resources)**. (1989) *Regional Geology of Liaoning Province*. Beijing: Geological Publishing House, pp. 856.
- Li QL, Wu FY, Li XH, Qiu ZL, Liu Y, Yang YH and Tang GQ** (2011) Precisely dating Paleozoic kimberlites in the North China Craton and Hf isotopic constraints on the evolution of the subcontinental lithospheric mantle. *Lithos* **126**, 127–34.
- Li SZ and Zhao GC** (2007) SHRIMP U–Pb zircon geochronology of the Liaoji granitoids: constraints on the evolution of the Paleoproterozoic Jiao-Liao-Ji belt in the Eastern Block of the North China Craton. *Precambrian Research* **158**, 1–16.
- Li Z, Ni LM and Xu JQ** (2016) The upper Proterozoic-Paleozoic records of sedimentary sequences and detrital zircon geochronology in Korean Peninsula and North China. *Acta Petrologica Sinica* **32**, 3139–54 (in Chinese with English abstract).
- Liu FL, Liu PH, Wang F, Liu CH and Cai J** (2015) Progresses and overviews of voluminous meta-sedimentary series within the Paleoproterozoic Jiao-Liao-Ji orogenic/mobile belt, North China Craton. *Acta Petrologica Sinica* **31**, 2816–46 (in Chinese with English abstract).
- Lu XP, Wu FY, Guo JH, Wilde SA, Yang JH, Liu XM and Zhang XO** (2006) Zircon U–Pb geochronological constraints on the Paleoproterozoic crustal evolution of the Eastern block in the North China Craton. *Precambrian Research* **146**, 138–64.
- Ludwig KR** (2003) *ISOPLOT 3.0: a Geochronological Toolkit for Microsoft Excel*. Berkeley: Berkeley Geochronology Center, Special Publications 4.
- Luo Y, Sun M, Zhao GC, Li SZ, Xu P, Ye K and Xia XP** (2004) LA-ICP-MS U–Pb zircon ages of the Liaohe Group in the Eastern Block of the North China Craton: constraints on the evolution of the Jiao-Liao-Ji Belt. *Precambrian Research* **134**, 349–71.
- Luo Y, Sun M, Zhao G, Li S, Ayers JC, Xia X and Zhang J** (2008) A comparison of U–Pb and Hf isotopic compositions of detrital zircons from the North and South Liaohe Groups: constraints on the evolution of the Jiao-Liao-Ji Belt, North China Craton. *Precambrian Research* **163**, 279–306.
- Metcalf I** (2006) Palaeozoic and Mesozoic tectonic evolution and palaeogeography of East Asian crustal fragments: the Korean Peninsula in context. *Gondwana Research* **9**, 24–46.
- Mitchell RH** (1986) *Kimberlites: Mineralogy, Geochemistry, and Petrology*. New York: Plenum Press, pp. 442.
- Oh CW** (2006) A new concept on tectonic correlation between Korea, China and Japan: histories from the late Proterozoic to Cretaceous. *Gondwana Research* **9**, 47–61.
- Oh CW, Imayama T, Lee SY, Yi S-B, Yi K and Lee BC** (2015) Permo-Triassic and Paleoproterozoic metamorphism related to continental collision in Yangpyeong, South Korea. *Lithos* **216–7**, 264–84.
- Paek RJ, Kang HG and Jon GP** (1996) *Geology of Korea*. Pyongyang: Foreign Languages Books Publishing House, 619 p.
- Parrish RR and Reichenbach I** (1991) Age of xenocrystic zircon from diatremes of western Canada. *Canadian Journal of Earth Sciences* **28**, 1232–8.
- Peng P, Wang C, Yang JH and Kim JN** (2016) A preliminary study on the rock series and tectonic environment of the ~1.9 Ga plutonic rocks in DPR Korea. *Acta Petrologica Sinica* **32**, 2993–3018 (in Chinese with English abstract).
- Peng P, Zhai MG, Li Q, Wu F, Hou Q, Li Z, Li T and Zhang Y** (2011) Neoproterozoic (~900Ma) Sariwon sills in North Korea: geochronology, geochemistry and implications for the evolution of the south-eastern margin of the North China Craton. *Gondwana Research* **20**, 243–54.
- Qiao XF and Zhang AD** (2002) North China block, Jiao-Liao-Korea block and Tanlu fault. *Geology in China* **29**, 337–45 (in Chinese with English abstract).
- Ree JH, Cho M, Kwon ST and Nakamura E** (1996) Possible eastward extension of Chinese collision belt in South Korea: the Imjingang belt. *Geology* **24**, 1071–4.
- Robles-Cruz SE, Escayola M, Jackson S, Galí S, Pervov V, Watangua M, Gonçalves A and Melgarejo JC** (2012) U–Pb SHRIMP geochronology of zircon from the Catoca kimberlite, Angola: implications for diamond exploration. *Chemical Geology* **310–11**, 137–47.
- Rollinson H**. 1997. Eclogite xenoliths in west African kimberlites as residues from Archaean granitoid crust formation. *Nature* **389**, 173–76.
- Rubatto D** (2002) Zircon trace element geochemistry: distribution coefficients and the link between U–Pb ages and metamorphism. *Chemical Geology* **184**, 123–38.
- Smith CB** (1983) Pb, Sr and Nd isotopic evidence for sources of southern African Cretaceous kimberlites. *Nature* **304**, 51–4.
- Sparks RSJ** (2013) Kimberlite Volcanism. *Annual Review of Earth and Planetary Sciences* **41**, 497–528.
- Sun J, Liu CZ, Tappe S, Kostrovitsky SI, Wu FY, Yakovlev D, Yang YH and Yang JH** (2014) Repeated kimberlite magmatism beneath Yakutia and its relationship to Siberian flood volcanism: insights from in situ U–Pb and Sr–Nd perovskite isotope analysis. *Earth and Planetary Science Letters* **404**, 283–95.
- Sun J, Tappe S, Kostrovitsky SI, Liu CZ, Skuzovatov SY and Wu FY** (2018) Mantle sources of kimberlites through time: A U–Pb and Lu–Hf isotope study of zircon megacrysts from the Siberian diamond fields. *Chemical Geology* **479**, 228–40.
- Sun SS and McDonough WF** (1989) Chemical and isotopic systematics of oceanic basalts: implications for mantle composition and processes. In *Magmatism in the Ocean Basins* (eds AD Saunders and MJ Norry), pp. 313–45. London: Geological Society, Special Publication no. 42.
- Valley JW, Kinny PD, Schulze DJ and Spicuzza MJ** (1998) Zircon megacrysts from kimberlite: oxygen isotope variability among mantle melts. *Contributions to Mineralogy and Petrology* **133**, 1–11.
- Wang HC, Ren YW, Lu SN, Kang JL, Chu H and Yu HB** (2015) Stratigraphic units and tectonic setting of the Paleoproterozoic Liao-Ji Orogen. *Acta Geologica Sinica* **36**, 583–98 (in Chinese with English abstract).
- Woodhead J, Hergt J, Shelley M, Eggins S and Kemp R** (2004) Zircon Hf-isotope analysis with an excimer laser, depth profiling, ablation of complex geometries, and concomitant age estimation. *Chemical Geology* **209**, 121–35.
- Wu FY, Han RH, Yang JH, Wilde SA, Zhai MG and Park SC** (2007a) Initial constraints on the timing of granitic magmatism in North Korea using U–Pb zircon geochronology. *Chemical Geology* **238**, 232–48.
- Wu FY, Li QL, Yang JH, Kim JN and Han RH** (2016) Crustal growth and evolution of the Rannim Massif, northern Korean Peninsula. *Acta Petrologica Sinica* **32**, 2933–47 (in Chinese with English abstract).
- Wu FY, Yang JH, Wilde SA, Liu XM, Guo JH and Zhai MG** (2007b) Detrital zircon U–Pb and Hf isotopic constraints on the crustal evolution of North Korea. *Precambrian Research* **159**, 155–77.
- Wu FY, Yang YH, Xie LW, Yang JH and Xu P** (2006) Hf isotopic compositions of the standard zircons and baddeleyites used in U–Pb geochronology. *Chemical Geology* **234**, 105–26.
- Wyllie PJ** (1980) The origin of kimberlite. *Journal of Geophysical Research: Solid Earth* **85**, 6902–10.
- Xie LW, Yang JH, Wu FY, Yang YH and Wilde SA** (2011) PbSL dating of garnet and staurolite: constraints on the Paleoproterozoic crustal evolution of the Eastern Block, North China Craton. *Journal of Asian Earth Sciences* **42**, 142–54.
- Yang JH, O'Reilly S, Walker RJ, Griffin W, Wu FY, Zhang M and Pearson N** (2010) Diachronous decratonization of the Sino-Korean craton: geochemistry of mantle xenoliths from North Korea. *Geology* **38**, 799–802.
- Yang JH, Peng P, Jong CS, Park U, Mun JG, Kim CH and Ku HC** (2016) Comparison on ages of detrital zircons from the Paleoproterozoic to Lower Paleoproterozoic sedimentary rocks in the Pyongnam Basin, Korea. *Acta Petrologica Sinica* **32**, 3155–79.
- Yang JH, Wu FY, Xie LW and Liu XM** (2007) Petrogenesis and tectonic implications of Kuangdonggou syenites in the Liaodong Peninsula, east North China Craton: constraints from in-situ zircon U–Pb ages and Hf isotopes. *Acta Petrologica Sinica* **23**, 263–76.
- Yin A and Nie S** (1993) An indentation model for the North and South China collision and the development of the Tan-Lu and Honam Fault Systems, eastern Asia. *Tectonics* **12**, 801–13.

- Zhai MG, Guo JH, Li Z, Chen DZ, Peng P, Li TS, Hou QL and Fan QC (2007b) Linking the Sulu UHP belt to the Korean Peninsula: evidence from eclogite, Precambrian basement, and Paleozoic sedimentary basins. *Gondwana Research* **12**, 388–403.
- Zhai MG, Guo JH, Li Z, Chen DZ, Peng P, Li TS, Zhang YB, Hou QL, Fan QC and Hu B (2007c) Extension of the Sulu UHP belt to the Korean Peninsula: evidence from orogenic belts, Precambrian basements, and Paleozoic sedimentary basins. *Geological Journal of China Universities* **13**, 415–28 (in Chinese with English abstract).
- Zhai MG, Guo JH, Peng P and Hu B (2007a) U–Pb zircon age dating of a rapakivi granite batholith in Rangnim massif, North Korea. *Geological Magazine* **144**, 547–52.
- Zhai MG, Zhang YB, Zhang XH, Wu FY, Peng P, Li QL, Hou QL, Li TS and Zhao L (2016) Renewed profile of the Mesozoic magmatism in Korean Peninsula: regional correlation and broader implication for cratonic destruction in the North China Craton. *Science China Earth Sciences* **59**, 2355–88.
- Zhang XH, Zhang YB, Zhai MG, Wu FY, Hou QL and Yuan LL (2016) Decoding Neoproterozoic to Palaeoproterozoic tectonothermal events in the Rangnim Massif, North Korea: regional correlation and broader implications. *International Geology Review* **59**, 16–28.
- Zhao GC, Cao L, Wilde SA, Sun M, Choe WJ and Li SZ (2006) Implications based on the first SHRIMP U–Pb zircon dating on Precambrian granitoid rocks in North Korea. *Earth and Planetary Science Letters* **251**, 365–79.
- Zhao GC, Sun M, Wilde SA and Li SZ (2005) Late Archean to Paleoproterozoic evolution of the North China Craton: key issues revisited. *Precambrian Research* **136**, 177–202.
- Zhao GC, Wilde SA, Cawood PA and Lu L (1998) Thermal evolution of Archean basement rocks from the eastern part of the North China Craton and its bearing on tectonic setting. *International Geology Review* **40**, 706–21.
- Zhao GC, Wilde SA, Cawood PA and Sun M (2001) Archean blocks and their boundaries in the North China Craton: lithological, geochemical, structural and PT path constraints and tectonic evolution. *Precambrian Research* **107**, 45–73.
- Zhao GC and Zhai MG (2013) Lithotectonic elements of Precambrian basement in the North China Craton: review and tectonic implications. *Gondwana Research* **23**, 1207–40.
- Zhao L, Zhang YB, Yang JH, Han RH and Kim JN (2016a) Archean rocks at the southeastern margin of the Rangnim massif, northern Korean, and their response to Paleoproterozoic tectonothermal event. *Acta Petrologica Sinica* **32**, 2948–64 (in Chinese with English abstract).
- Zhao L, Zhang YB, Wu FY, Li QL, Yang JH, Kim JN and Chou WJ (2016b) Paleoproterozoic high temperature metamorphism and antesis in the northern Korean Peninsula: constraints from petrology and zircon U–Pb geochronology. *Acta Petrologica Sinica* **32**, 3045–69 (in Chinese with English abstract).
- Zheng JP, Griffin WL, O'Reilly SY, Yu CM, Zhang HF, Pearson N and Zhang M (2007) Mechanism and timing of lithospheric modification and replacement beneath the eastern North China Craton: peridotitic xenoliths from the 100 Ma Fuxin basalts and a regional synthesis. *Geochimica et Cosmochimica Acta* **71**, 5203–25.
- Zheng JP, Griffin WL, O'Reilly SY, Zhang M, Pearson N and Pan Y (2006) Widespread Archean basement beneath the Yangtze craton. *Geology* **34**, 417–20.
- Zheng JP, Griffin WL, O'Reilly SY, Zhao JH, Wu YB, Liu GL, Pearson N, Zhang M, Ma CQ, Zhang ZH, Yu CM, Su YP and Tang HY (2009) Neoproterozoic (2.7–2.8 Ga) accretion beneath the North China Craton: U–Pb age, trace elements and Hf isotopes of zircons in diamondiferous kimberlites. *Lithos* **112**, 188–202.